ISSN 1330-3651 (Print), ISSN 1848-6339 (Online) https://doi.org/10.17559/TV-20240610001765
Original scientific paper

Investigation of Tribological Performance cum Machining Efficiency with Surface Quality of Al HMMC Reinforced with ES-Gr using GRA and SEM Outcomes

M. DHANENTHIRAN*, C. BALAMURUGAN, A. BOVAS HERBERT BEJAXHIN

Abstract: The aerospace, industrial, and automotive sectors employ metal matrix composites (MMCs) because of their low mass, high strength, and structural stiffness. This study built AA6061-graphite and AA6061-graphite-eggshell hybrid composites to compare their mechanical properties to the alloy. Reinforcement pre-heating temperatures of 900 °C and stir casting generated AA6061 samples reinforced with eggshell powder volumes of 0–5% and 5% graphite volumes. A pin-on disc tribometer was adjusted to assess wear. These parameters were *Gr* and *Es* weight percentage (0% to 5%), applied load (20 N to 40 N), speed (150 rpm to 450 rpm), and duration (5 to 15 minutes). The optimal wear process parameters for wear resistance are found by using response surface techniques. The results showed that alloys and composites' wear rates increased with applied load and speed. Tensile, hardness, and compression tests were utilized to assess mechanical properties, and graphite and egg shell reinforcement changed the findings. Graphite and eggshell enhance the hardness, tensile strength, and compressive strength of a substance. The results indicated that the mechanical properties of reinforced materials might be enhanced. Three significant variables determined the optimization method: feed rate (0.10 - 0.15 mm/rev), spindle speed (850 - 1050 rpm), and depth of cut (0.30 - 0.90 mm). Responses to Metal Removal Rate, Surface Roughness, and Machining Time were investigated in the optimization study. GRA optimized Taguchi's L9 orthogonal array was utilized to execute the experimental design. The optimum cutting speed, feed rate, and depth of cut for this hybrid composite were 1050 rpm, 0.15 mm per revolution, and 0.6 mm, respectively.

Keywords: grey relation analysis; hybrid metal matrix composite; mechanical properties; reinforcement; stir casting; tribological behaviour

1 INTRODUCTION

Composites of aluminium matrix metal have widening of structural applications across productions such as automobile, aircraft, sports, and defence. In sophisticated industrial applications, hybrid composites comprising a minimum of two reinforcements may be employed. The characteristics of composites are determined by the matrix, reinforcement, and refining parameters that are utilized [1, 8]. The composite materials properties are significantly compromised by the addition of large quantities of reinforcing particulates. The maximum strengths attained were as follows: tension of 175 MPa, hardness of 45 HRB, ZrO2 content of 4.56E-9 g/mm, and C content of 2 wt% [2]. Aluminium-based metal matrix composites exhibit superior performance compared to monolithic alloys and microparticle-reinforced composites. Density was increased by the incorporation of SiC and MOS2 into the reinforced Al6061 composite. The stiffness of a mixed metal matrix composite increased with the quantity of B4C present [3]. Most research indicates that augmenting the reinforcing particles results in enhanced mechanical and tribological characteristics of the composites [4]. In order to enhance understanding of the AA6061 alloy's tribological and mechanical properties, further research should be conducted on boron carbide reinforcement. The researchers utilized stir casting to fabricate innovative aluminum metal matrix composites by incorporating three distinct percentages of reinforcement by weight of B4C: 5%, 10%, and 15%. The samples have exhibited improved mechanical properties, as indicated by their heightened shear strength, resistance to impact testing, and significant deformation. [6]. A study indicates that the mechanical properties of a hybrid composite comprising 4% molybdenum disulphide and 4% graphite particles are superior to those of conventional composites. By utilizing stir casting, aluminium metal matrix composites with a hybrid composition were produced. Microstructural imaging is employed to verify the uniform distribution of graphite and MoS_2 reinforcement throughout the surface. [7]. The samples received 2% silicon nitride (Si_3N_4), and 5% eggshell as reinforcements. According to the results, it is possible to enhance the mechanical characteristics of reinforced materials [9]. A comprehensive evaluation was conducted on the tribology behaviour, density, rigidity, and compression strength of the aluminium matrix nano composite prior to and following heated isostatic pressing (HIP). A reduction in density of 38% was observed in nanocomposites lacking HIP; nevertheless, the incorporation of HIP resulted in a density decrease of 45%. HIP decreases friction coefficient by 45%, whereas B4C and CNTs decrease it by 20% overall, but only by 48% in nanocomposites [10, 17]. The final products of aluminium composites have enhanced tribological properties, hardness, rigidity, strength, and a greater strength-to-weight ratio expected to be useful for heat exchanger and heat sink application [5, 11]. As AMMC reinforcements, the use of ecological, decomposable materials such as agri refuse is investigated. Their potential application as engine component materials is investigated. The results indicate that they are capable of substantial weight and financial savings [12]. Particle reinforcements including silicon, aluminium oxide, graphite, boron carbide, titanium carbide, fly dust, bagasse dust, and red sediment were incorporated into the Al-6061 alloy via stir casting. The reinforcements were arranged in the form of single, dual, and triple strands. The experimental findings indicated that the mechanical and tribological properties of Al-6061 metal matrix composites were considerably superior to those of the Al-6061 alloy. [13]. The findings showed that a growth in the quantity of reinforcement particles directed to a concomitant enhancement in hardness, ultimate and yield strength, in contrast to the Al6061 alloy. Nevertheless, the elongation values decreased. Small flaws were observed in both the unreinforced alloy and the composite, as determined by fractography [14]. An investigation demonstrates that agro-waste materials have the potential to serve as reinforcing materials in lieu of the conventional boron carbide and silicon carbide. This research employs clay particles and rice husk ash owing to their demonstrated ability to enhance composite properties such as hardness, tension, and bending strength [15]. Utilizing powder metallurgy, this study investigates the characteristics of magnesium alloy-based composites fortified with hydroxyapatite (HA). Several techniques were utilized to examine the composites, such as SEM, EDS, and XRD. The findings indicated that the Mg3Al/9HA composite exhibited enhanced mechanical strength and improved resistance to attrition. The parameters that yielded the lowest attrition rate and friction coefficient were determined to be 9 weight percent, 1 meter per second, 750 meters, and 5 N [16]. These findings could guide material selection and application in industries like automotive, industrial, and aerospace. Therefore, the effect of graphite and egg shell particle reinforcement in stir cast metal matrix composites composed of Al6061 alloy was investigated in the current study. Samples of AA6061 reinforced with varying concentrations of eggshell volume (0, 5%) and a constant volume of graphite (5%) were manufactured by stir casting at 900 °C for the reinforcement preheating process. Utilizing response surface methodologies to determine the optimal wear process parameters for resistance to wear. The mechanical properties of the material were evaluated through the implementation of tension, hardness, and compression testing. The outcomes of these tests were found to be affected by the incorporation of reinforcement material additives, such as egg shell and graphite. Using CNC turning, the optimization method was determined by three critical parameters: spindle speed, feed rate, and depth of cut. The optimization study investigated the responses of *MRR*, *Ra*, and *MT*. [18] The effects of wire electrical discharge machining (WEDM) parameters on the tribological and microstructural properties of SiC-Gr reinforced Al2219 composites were investigated by Babu et al. (2023). Their study revealed that the optimization of WEDM constraints significantly enhances the wear resistance and structural integrity of the composites. Detailed microstructural analysis supported these findings, showing improved bonding and reduced defects. [19] Prabakaran et al. (2024) investigated the development and strength evaluation of eco-friendly natural fiber composites using tribological methods and scanning electron microscopy (SEM). Their research demonstrated that these composites exhibit superior tribological properties and mechanical strength, attributed to the optimized experimental conditions. The SEM images provided insights into the microstructural improvements achieved through their methodology. [20] Bejaxhin et al. (2021) The tribological behavior and surface roughness of dual heat-treated Al6061 composites were analyzed using CNC milling. By combining graphite and eggshell, we aimed to leverage the lubricating properties of graphite and the stiffness and sustainability of eggshell. This hybrid reinforcement approach optimizes the composite for mechanical strength, wear resistance, and environmental sustainability, aligning with current demands in industrial, automotive, and aerospace applications.

2 MATERIALS

For their substantial structural functions, aluminium metal matrix composites are widely employed in the automotive, aerospace, sports, and defence industries. Hybrid composites, comprising two or more reinforcements, find utility in intricate industrial contexts. The properties of the composites are reliant on the precise combination of matrix material, reinforcing agent, and fabrication parameters.

2.1 AA6061

Due to its remarkable attributes, which include moderate to high strength, exceptional resistance to environmental factors, low density, high elongation at break, and excellent machinability, Al-6061 is widely employed in the 6000-aluminum series. Tab. 1 presents the chemical composition of AA6061 alloy. It is a matrix that is commonly employed in the fabrication process of aluminium matrix composites (AMCs). AA6061 was selected for its favourable strength-to-weight ratio, corrosion resistance, and simplicity of machinability, all of which are essential for applications in the aerospace and automotive industries. Furthermore, AA6061 demonstrates excellent compatibility with reinforcements, enabling the successful integration of graphite and eggshell particles. This results in a hybrid composite with improved properties that retains the advantages of the aluminum alloy matrix.

Table 1 Chemical composition of AA6061 alloy (wt%)

Constituent element	Weight / %	
	Min	Max
Al	95.85%	98.56%
Mg	0.80%	1.20%
Si	0.40%	0.80%
Fe	0	0.70%
Cu	0.15%	0.40%
Cr	0.04%	0.35%
Zn	0	0.25%
Ti	0	0.15%
Mn	0	0.15%

2.2 Graphite

Graphite is a carbon-based substance that has a crystalline structure composed of closely packed carbon atoms arranged in layers or sheets. Consequently, graphite exhibits fragility when subjected to shearing forces parallel to its layers. Graphite possesses low frictional properties due to its characteristic of being a solid lubricant. Graphite exhibits abrasive properties and has limited lubricating abilities in a vacuum. However, its frictional qualities are only reduced when exposed to air or moisture. Graphite exhibits a unique property where its strength and stiffness enhance as the temperature rises, setting it apart from other materials. Graphite is well-suited for nuclear applications because of thermal neutrons, it exhibits a high scattering cross section and a decreased absorption cross section.

2.3 Egg Shell

95 - 97% of the biogenic solids in eggshells are calcium carbonate. When compared to artificial calcium carbonate, the range of CaCO3 is smaller. CaCO3 is often used because of its remarkable ability to serve as an MMC reinforcement. Making eggshell powder is a tedious process that takes a long time to complete. After the eggshells were thoroughly cleaned to remove the membrane, they were placed on a circular stainless-steel tray and allowed to air dry for six hours. Before being removed from the mill, the dry eggshells were first finely ground in a planetary ball mill for three hours after being crushed by hand compression. Sieves with the designated mesh size were used to filter the resultant powder to produce particles with a consistent size distribution. Material Density and Properties are given in Tab. 2.

Table 2 Material density and properties

S. No.	Material	Density / g/cc	Properties
MATRIX			
1	AA6061	2.810	superior thermal properties, better tensile strength.
REINFORCEMENTS			
1	Graphite / *Gr*	2.26	Hard Ceramic - improve hardness, Wear resistance, strong interfacial bonding, low coefficient of thermal expansion, better wettability with aluminium matrix.
2	Eggshell Powder / Es	2.5	low density, renewable high thermal stability

3 EXPERIMENTATION
3.1 Fabrication of Composite

The Stir casting manufacturing process, illustrated in Fig. 1, is an economically viable and efficient method for fabricating metal matrix composites with aluminum serving as the foundational material. The matrix material used is AA6061, while the reinforcing elements consist of graphite and eggshell, the ration as shown in Tab. 3. Fig. 1 and Fig. 2 illustrate the final composites materials and AA6061 Aluminium hybrid composites with metal matrix by the stir casting approach. Preheating at this temperature facilitates superior bonding with the AA6061 matrix during stir casting, ensuring uniform dispersion of the reinforcement particles. This procedure is crucial to prevent weak points in the composite and to provide uniform mechanical characteristics throughout the material.

Table 3 Sample composition

Samples	Al Alloy 6061 / %	Graphite	Egg Shell
Ratio 1	100	-	-
Ratio 2	95	5%	-
Ratio 3	90	5%	5%

This pre-heating helps improve wettability and reduces porosity within the composite by reducing the likelihood of particle agglomeration. Exactly 650 grams of AA6061 is melted in a stir casting furnace. Reinforcing particles that have been heated beforehand are added slowly to the molten aluminum while it is being stirred at a rate of 600 revolutions per minute. The amalgamated molten substance is introduced into the cast aluminium mold at a temperature of 780 °C, yielding castings with a diameter of 30 mm and a length of 350 mm.

Figure 1 Stir casting machine

Figure 2 Composite specimen

3.2 Wear Behaviour

Under dry sliding conditions, the wear behaviour of the proposed Al/graphite/egg shell composite material was investigated to further evaluate its mechanical properties. Wear pegs measuring 50 mm in length and 10 mm in diameter were manufactured for this purpose. Aluminium (Al), Aluminium incorporating 5% graphite (Al/5Gr), and Aluminium incorporating 5% graphite and 5% egg shell powder (Al/5Gr/5Es) constitute the composites. The wear test was performed in accordance with the ASTM G99 standard. The utilized disc object was composed of EN 31. The material was hardened steel, measuring 90 mm in diameter and 8 mm in thickness. Utilized was a weighing balance with a resolution of 0.00001 g. The control variables, their respective levels, and the experimental conditions utilized in the wear test are illustrated in Tab. 4 and Tab. 5. These ranges represent standard operational circumstances, enabling us to assess the wear performance of the composite under authentic stress and velocity situations. Evaluating within these parameters yields pertinent information regarding the composite's durability and abrasion resistance. The pin-on-disc apparatus, more precisely the Ducom Wear test model, employs load cells to measure the tangential forces that operate upon specimens. The schematic of the pin-on-disc configuration is illustrated in Fig. 3 and the specimen in Fig. 4. Utilizing the wear data obtained from the specimens, the WR (Wear Rate) and *COF* (Coefficient of Friction) are calculated. Four control variables, each with three levels, were utilized in this study. By optimizing the wear factors, the objective was to achieve the minimum wear rate possible.

Figure 3 Pin on- disc wear test machine

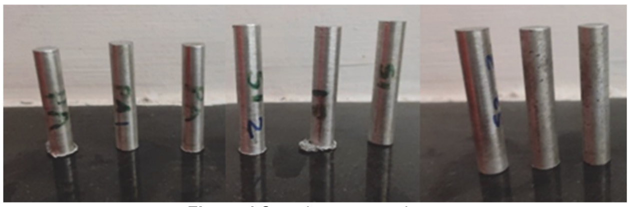

Figure 4 Sample wear specimen

Table 4 Dry sliding wear parameters and levels

Level	Parameters			
	Wt % Gr & Es	Applied Load / N	Speed / rpm	Time / min
1	0%	20	150	5
2	5%	30	300	10
3	10%	40	450	15

3.3 CNC Turning Operation

Additionally, the analysis may be conducted using the Taguchi method's L9 orthogonal array in CNC turning process. Fig. 5 and Fig. 6 depict the use of BATLIBOI smart run CNC lathe for the process of turning, with a reinforced composite material serving as the workpiece material. The workpiece has a length of 60 mm and a diameter of 26 mm. The investigation used a Carbide-TAEGUTEC-TT-5100-04 insert as the tool material. The Tab. 6 and Tab. 7 illustrate the examination of *MRR*, *Ra*, and *MT* at different input parameters, including feed rate, speed, and depth of cut.

Figure 5 CNC turning machine

Table 6 Identifying process parameters and their corresponding levels

Levels	Machining Parameters		
	Spindle Speed / rpm	Feed / mm/Rev	Depth of Cut / mm
1	850	0.100	0.3
2	950	0.125	0.6
3	1050	0.150	0.9

The Taguchi method determines the optimal parameter for attaining desired outcomes through the utilization of qualitative and experimental observations. The Taguchi robust design is an exceptionally effective method for minimizing the quantity of required experiments. As shown in Tab. 6 and Tab. 7, the Machining Time (*MT*) for the L9 orthogonal array turning operation executed with CNC was determined using a timer. The TR-200 surface roughness analyzer was utilized to determine the surface roughness, *Ra*, whereas the weight approach was employed to compute the material removal rate, *MRR*. This approach allowed us to identify the optimal machining conditions with precision, ensuring the best balance of machining efficiency and material quality for the hybrid composite.

Table 5 Tribological experimental design (L27 orthogonal array)

Sl. No.	Weight % *Gr* & Es	Applied Load / N	Speed / rpm	Time / min	Specific Wear Rate × 10^{-2} / mm^3/Nm	Coefficient of Friction
1.	0	20	150	5	3.121	0.66
2.	0	20	150	10	4.238	0.69
3.	0	20	150	15	5.291	0.71
4.	0	30	300	5	9.212	0.53
5.	0	30	300	10	14.835	0.58
6.	0	30	300	15	23.012	0.62
7.	0	40	450	5	46.409	0.33
8.	0	40	450	10	64.238	0.41
9.	0	40	450	15	87.489	0.48
10.	5	20	300	5	2.821	0.41
11.	5	20	300	10	3.001	0.46
12.	5	20	300	15	4.182	0.48
13.	5	30	450	5	14.327	0.32
14.	5	30	450	10	21.563	0.35
15.	5	30	450	15	27.343	0.39
16.	5	40	150	5	17.732	0.53
17.	5	40	150	10	36.199	0.58
18.	5	40	150	15	48.029	0.63
19.	10	20	450	5	2.890	0.33
20.	10	20	450	10	3.538	0.35
21.	10	20	450	15	4.709	0.37
22.	10	30	150	5	7.903	0.49
23.	10	30	150	10	13.355	0.51
24.	10	30	150	15	19.611	0.55
25.	10	40	300	5	27.078	0.38
26.	10	40	300	10	36.199	0.42
27.	10	40	300	15	49.448	0.47

Table 7 CNC Turning (L9 orthogonal array) experimental design

Sl.No.	INPUT PARAMETERS			OUTPUT PARAMETERS		
	Spindle Speed / rpm	Feed / mm/Rev	Depth of Cut / mm	*MRR*	*Ra*	Machining Time
1.	850	0.100	0.30	0.152	3.733	52
2.	850	0.125	0.60	0.188	4.465	48
3.	850	0.150	0.90	0.222	7.333	39
4.	950	0.100	0.60	0.162	3.853	51
5.	950	0.125	0.90	0.210	3.986	43
6.	950	0.150	0.30	0.208	4.132	38
7.	1050	0.100	0.90	0.184	4.103	47
8.	1050	0.125	0.30	0.179	3.117	42
9.	1050	0.150	0.60	0.220	2.720	36

4 RESULTS AND DISCUSSION

The compressive and tensile strengths of the material were evaluated through mechanical testing using a universal testing apparatus (UTM 60 M/c 6/2007.3672) that had been precisely calibrated. The hardness evaluation was performed utilizing a Rockwell hardness tester.

4.1 Tensile Strength Values

Tensile testing is used to evaluate the mechanical properties of friction treated joints. Tab. 8 presents the outcome of the tensile strength test, which is used to assess several tensile properties including tension strength, strength of yield, and % of elongation. Tensile inspection is used to analyse hybrid aluminium composites in line with the ASTM standard. Fig. 7 illustrates the graphical depiction of tensile specimen values, demonstrating that the reinforcing materials exhibit greater tensile values compared to pure aluminium.

Table 8 Tensile strength value of the specimens

Sample	*YL* / kN	*YS* / N/mm^2	*TL* / kN	*TS* / N/mm^2	*E* / %
Ratio1	12.97	104.68	17.46	140.92	4.52
Ratio2	14.26	118.46	18.65	154.93	7.36
Ratio3	15.92	135.30	20.57	174.82	8.88

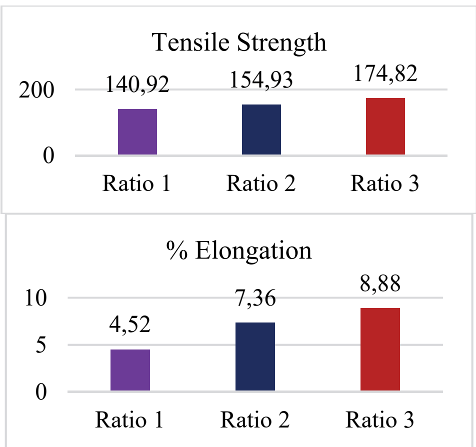

Figure 7 Graphical representation of tensile and % of elongation for tensile specimen

4.2 Compressive Strength Values

A compression test is a procedure in which a sample is subjected to opposing pressures that push inward from opposite sides, resulting in compression of the specimen. The objective of compression testing is to determine the compressive strength or resistance of a material. Tab. 9 illustrates the assessment of compression strength value. A compression test is conducted to evaluate the response of a material when subjected to a compressive force in Fig. 8. Aluminium composites are prepared for compression examination according to the ASTM standard.

Table 9 Compression strength test value

Sample	Compression load / KN	Compression Strength / N/mm^2
Ratio1	58.96	338.15
Ratio2	61.36	352.86
Ratio3	64.29	378.30

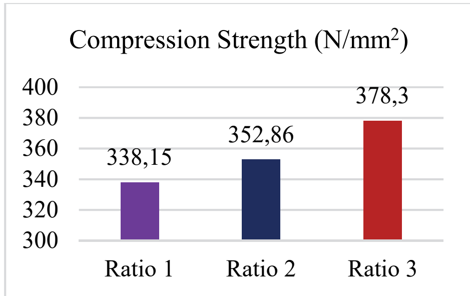

Figure 8 Graphical representation of compression strength specimen

4.3 Hardness Test Values

The values of 67 HRB for the Ratio 1 (pure alloy), 78 HRB for the Ratio 2 developed Aluminium composite (95% AA6061 + 5% *Gr*), and 87 HRB for the Hybrid Aluminium composite (90% AA6061 + 5% *Gr* + 5% Es) were obtained by measuring the hardness under a load of 100 Kgf with an indenter of 1/16' ball. The reinforced composite (Ratio 3) contributed to a 13% increase compared to pure aluminium (Ratio 1) in the hardness of aluminum composite, as shown in Tab. 10 and Fig. 9.

Table 10 Hardness test value (HRB)

Sample	Load / Kgf	Indenter	Scale	HRB
Ratio1	100	1/16' ball indenter	B	67
Ratio2				78
Ratio3				87

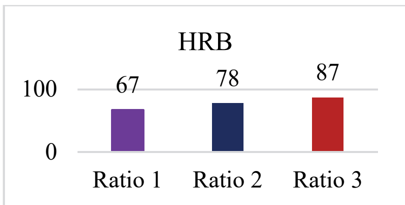

Figure 9 Graphical representation of hardness value

4.4 SEM Microstructure

The scanning electron microscopy (SEM) images shown in Fig. 10a to Fig. 10b showcase metal matrix composites that were produced by casting AA60601/5% *Gr*.

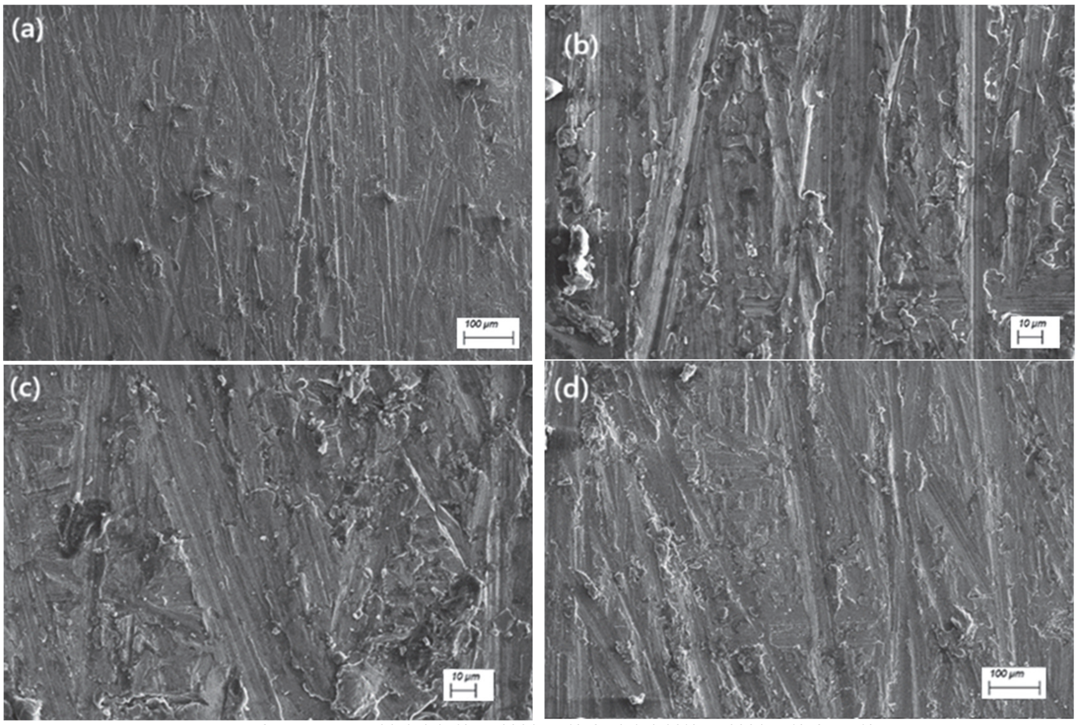

Figure 10 SEM imaging of (a&b) 95% AA6061 + 5% *Gr*; (c&d) 90% AA6061+ 5% *Gr* + 5% Es

The distribution of graphite (*Gr*) particles in the grain boundary of the AA60601/5% *Gr* matrix is uniformly shown in each picture. These images provide visual evidence of the uniform distribution of reinforcement particles within the matrix, which contributes to the improved mechanical properties and wear resistance observed in the composite. The occurrence of agglomeration is less prominent at greater proportions in the sample, as seen in Fig. 10c to Fig 10d. To obtain a uniform distribution, it is crucial to ensure the accurate casting of aluminum, graphite, and Eggshell powder. Achieving desirable mechanical and attrition properties requires the careful and precise distribution of graphite and eggshell particles. Achieving a homogeneous distribution of graphite and eggshell particles is crucial for obtaining optimal mechanical and wear characteristics.

5 EXPERIMENTAL DATA ANALYSIS AND OPTIMIZATION

5.1 Taguchi Technique for Dry Sliding Wear

The ANOVA findings in the Tab. 11 indicate that the applied load is the most important parameter in influencing wear, contributing 69% to the overall effect. The weight percentage accounts for 10% of the wear rate reduction, followed by time at 7% and speed at 9% and the *R*-Square of 89.88% in Tab. 12

The relationship between wear rate and applied load. The study concludes that the applied load significantly affects the wear rate of both pure aluminum alloy and hybrid composite. The correlation between the wear rate and applied load indicates that Archard's law is being followed in this case. By focusing on wear rate reduction, the optimization process aimed to identify conditions that maximized the composite's wear resistance. Based on Fig. 11a to Fig. 11d, it is evident that an escalation in wear rate occurs as the applied load increases. However, it is noteworthy that the hybrid composite exhibits a lower wear rate compared to aluminum. Both Aluminum and hybrid composite specimens have an elevated wear rate when their speed is increased, attributed to a rise in temperature at the contact point. An increase in speed results in a drop-in wear rate in hybrid composite materials, whereas an increase in wear rate is seen in aluminum. The Fig. 12 illustrates the interaction plot for the wear rate, with the combination of load and weight percentage of *Gr* & *Es* being the most influential elements.

Table 12 Model summary for specific wear rate

S	*R*-sq	*R*-sq(*adj*)	*R*-sq(*pred*)
8.25898	89.88%	85.38%	77.23%

Table 11 Analysis of variance for specific wear rate

Source	D*F*	Seq *SS*	Seq *MS*	*F*-Value	*P*-Value	Contribution / %
Weight % *Gr* & Es	2	1227.8	613.9	19.111	0.0003	10%
Applied Load / N	2	8367	4183.5	130.236	0	69%
Speed / rpm	2	905.6	452.8	14.096	0.0002	7%
Time / Min	2	1052.9	526.45	16.388	0.0001	9%
Error	18	578.2	32.122			5%
Total	26	12131.5				

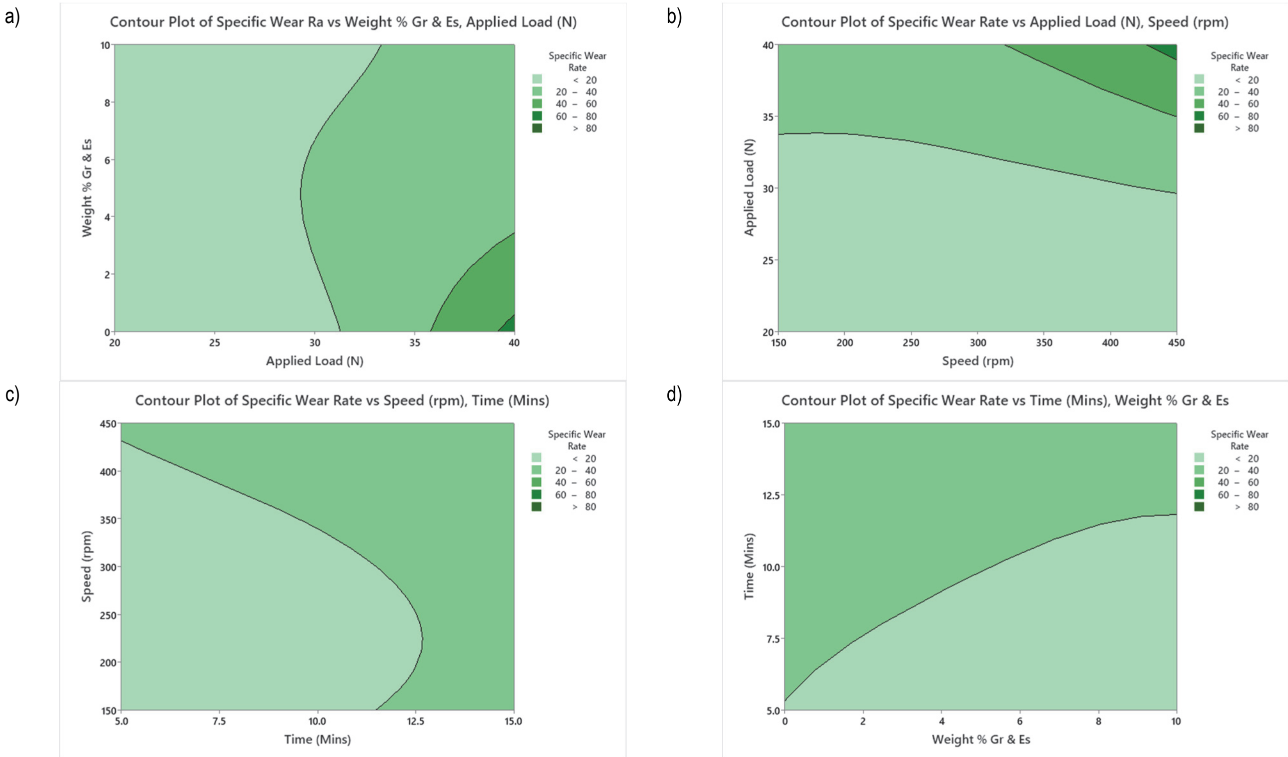

Figure 11 Contour-plot image for dry sliding wear

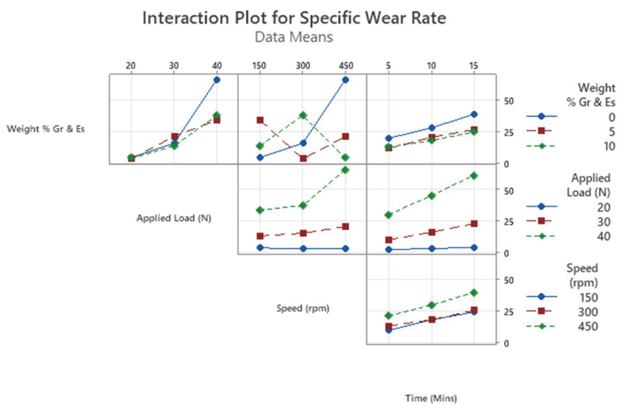

Figure 12 Interaction plot image for dry sliding wear

5.2 Taguchi Technique for Coefficient of Friction

The control parameter that has the greatest influence on the coefficient of friction is speed, Tab. 13 shows accounting for 65% of the overall contribution. Weight percentage is the next most important factor, contributing 22%. Time and applied load have smaller impacts, with contributions of 8% and 1% respectively, and the *R*-Square of 96.05% in Tab. 14

The Fig. 13e to Fig. 13h displays the coefficient of friction (*COF*) as a function of the weight percentage of graphite (*Gr*) and epoxy resin (*Es*) vs the applied load, the applied load versus the speed, the speed versus time, and the time versus the weight percentage of graphite (*Gr*) and epoxy resin (*Es*). During the wear testing of composite materials, the coefficient of friction (*COF*) demonstrates a positive correlation with the applied load, meaning that as the load increases, the *COF* also increases. The suggested materials exhibit greater wear resistance due to many aspects. These include their hardness, higher graphite and egg shell content in the aluminium alloy, and inherent wear resistance.

Table 13 Analysis of variance for co-efficient of friction

Source	DF	Seq *SS*	Seq *MS*	*F*-Value	*P*-Value	Contribution / %
Weight % *Gr* & *Es*	2	0.078	0.039	50.99	0	22%
Applied Load / N	2	0.003	0.001	1.91	0.177	1%
Speed / rpm	2	0.226	0.113	147.37	0	65%
Time / min	2	0.028	0.014	18.73	0	8%
Error	18	0.013	0.0007			4%
Total	26	0.350				

Table 14 Model summary for co-efficient of friction

S	*R*-sq	*R*-sq(*adj*)	*R*-sq(*pred*)
0.0277333	96.05%	94.30%	91.12%

The interaction plot shows the influence of regulating factors on performance characteristics, specifically highlighting the minimal coefficient of friction (*COF*) when the reinforcement level is high and the load is low. The influence of the weight percentage of *Es* and *Gr* on the coefficient of friction (*COF*) is readily evident from the interaction plot in Fig. 14 when considering the other parameters. The *Es* particles function as a wear-resistant agent inside the matrix materials. In this study, it was shown that the interaction of Load had a stronger impact compared to the other factors examined, in terms of weight percentage (Wt %). This is because the load causes deformation on the samples.

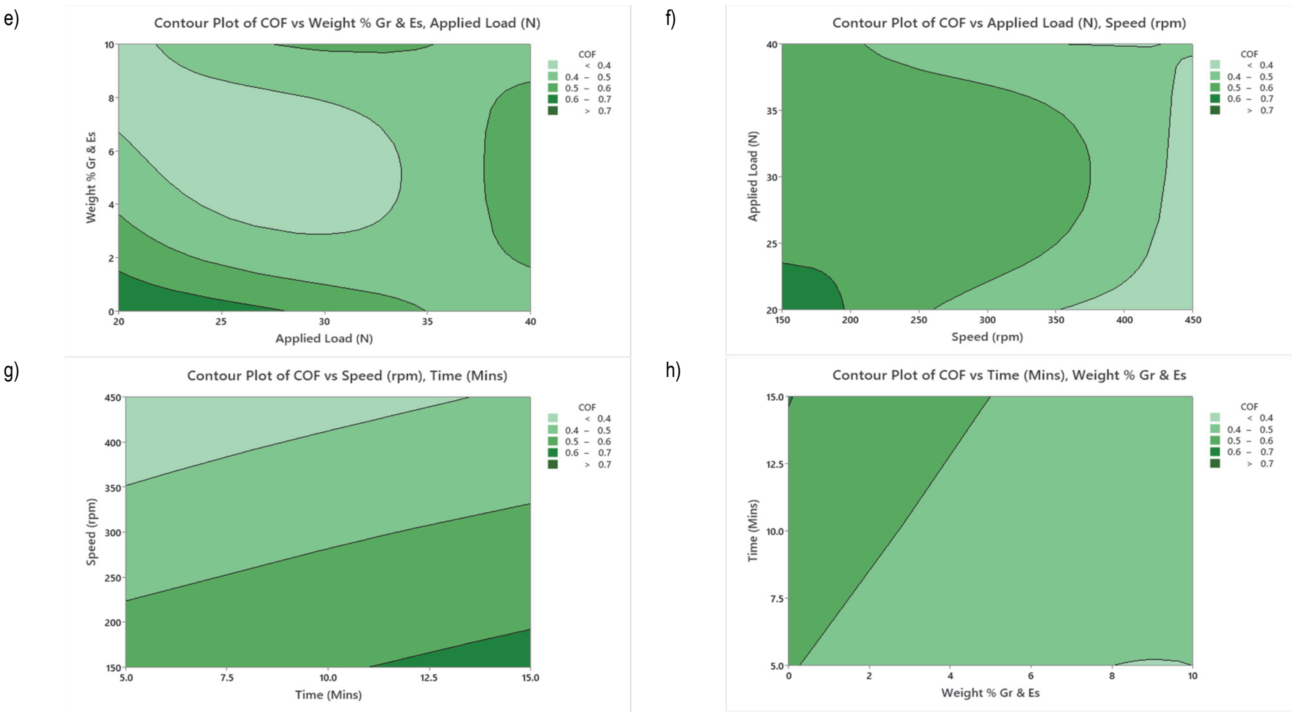

Figure 13 Contour-plot image for co-efficient of friction

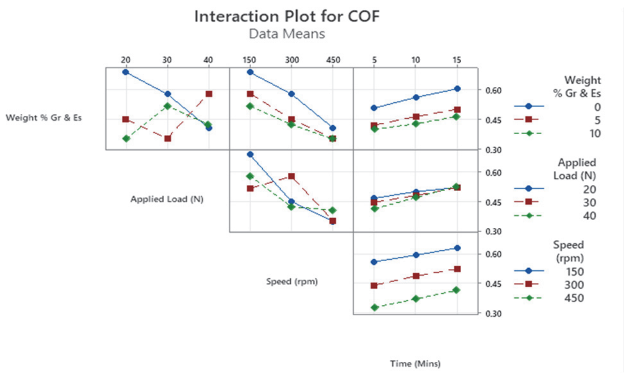

Figure 14 Interaction plot image for co-efficient of friction

5.3 Grey Relation Generation for CNC Turning Parameters of Hybrid Composite Material

The greatest grades of gray relations are designated with a rank of 1. Equations are utilized to compute gray relational grades, while Tab. 15 is consulted to ascertain the grey relational order. Based on the information in Tab. 15, it was determined that the grey relational grade was greatest when the control parameter was set to its maximum speed.

Table 16 Mean values of grade (manual calculation)

Grey Relation Grade - Response Table					
Parameter	level 1	level 2	level 3	Mean effect	Rank
Speed	0.544	0.605	0.705	0.161	2
Feed	0.475	0.586	0.645	0.171	1
Depth of Cut	0.597	0.645	0.612	0.049	3

Table 17 Taguchi analysis: GRG versus SPEED, FEED, DEPTH OF CUT

Response Table for Means			
Level	SPEED	FEED	DEPTH OF CUT
1	0.5443	0.4749	0.5966
2	0.6050	0.5859	0.6455
3	0.7050	0.7935	0.6122
Delta	0.1607	0.3186	0.0489
Rank	2	1	3

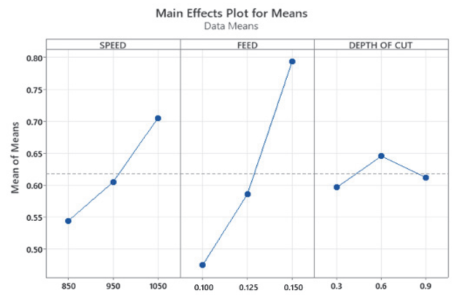

Figure 15 Main effects plot for means

Based on the analysis of the nine experiments considered, it can be inferred that the S3F3D2 setting produced the highest *MRR*, minimal surface roughness, and shortest machining time. illustrated in Fig. 16, demonstrates that the input rate exerts the greatest influence, with speed following suit. The degree of uniformity exhibited by the samples is influenced by the feed rate.

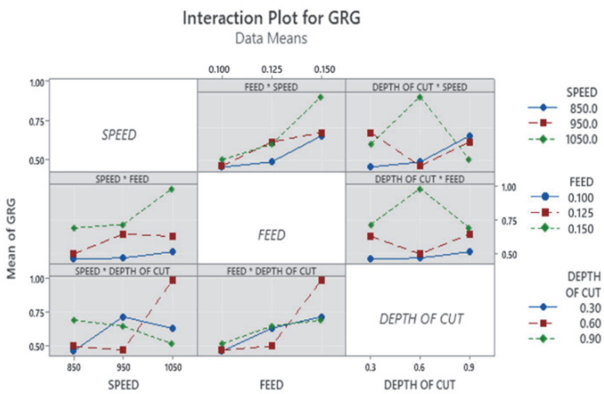

Figure 16 Interaction plot for GRG

The gray relational grade was assessed according to its signal-to-noise (S/N) quality attributes, which were larger and more favorable, to attain enhanced performance across various characteristics. The parameter level that produces the optimal signal-to-noise ratio is regarded as the optimal value. It was ascertained that the optimal process parameter configuration for the multiple performance characteristic is s3f3d2. Tab. 16 and Tab. 17 present the principal effects plot pertaining to the mean of GRG from manual calculation as well as mini tab softwares, while Fig. 15 depicts the same plot. The interaction plot for GRG, as

Table 15 Grey relation coefficient and grade

Sl.No.	Input Parameters			Grey Relational Coefficient			GRG	Rank
	SPEED	FEED	DOC	*MRR*	*Ra*	Machining Time		
1.	850	0.100	0.3	0.333	0.695	0.333	0.454	9
2.	850	0.125	0.6	0.507	0.569	0.400	0.492	7
3.	850	0.150	0.9	1.000	0.333	0.727	0.687	3
4.	950	0.100	0.6	0.368	0.671	0.348	0.462	8
5.	950	0.125	0.9	0.745	0.646	0.533	0.641	4
6.	950	0.150	0.3	0.714	0.620	0.800	0.712	2
7.	1050	0.100	0.9	0.479	0.625	0.421	0.509	6
8.	1050	0.125	0.3	0.449	0.853	0.571	0.624	5
9.	1050	0.150	0.6	0.946	1.000	1.000	0.982	1

5.4 Response Table from Minitab 21 Software

Tab. 18 represents the results of the ANOVA for the Grey relation grade. The primary contributor, with a 79.73% level of confidence, is the feed, followed by the depth of cut (3.71%) and speed (13.11%). The recorded error is 3.56%, which provides justification for the statement that the error is minimal and extremely reliable.

Table 18 Analysis of variance for GRG

Source	D*F*	Seq *SS*	Contribution	Adj *SS*	Seq *MS*	*F*-Value	*P*-Value
Speed	2	0.007014	13.01%	0.024601	0.012301	3.65	0.215
Feed	2	0.150814	79.73%	0.150814	0.075407	22.39	0.043
Depth of Cut	2	0.024601	3.71%	0.007014	0.003507	1.04	0.49
Error	2	0.006737	3.56%	0.006737	0.003368		
Total	8	0.189166	100.00%				

6 CONCLUSION

Microstructural characterization, tribological testing, mechanical analysis, and CNC turning machining were conducted on unreinforced AA6061 aluminium and aluminium reinforced with 5% graphite and 10% (5% graphite and 5% eggshell powder) particles, respectively, in the current study. The following conclusions were derived from the collected experimental results

Stir casting was utilized to effectively fabricate the AA6061/*Gr*/*Es* hybrid composite, and a uniform dispersion of reinforcement particles throughout the matrix was found. Compared to the unreinforced AA6061 alloy, the hybrid composite exhibited an 11.87% increase in hardness and a 24.05% improvement in compressive strength. These improvements suggest that the composite offers a notable advantage in durability and mechanical performance, which is critical for components subjected to high loads and friction.

The experimental findings indicate that the unreinforced alloy exhibited inferior wear resistance in comparison to the hybrid composite. It was found that the hybrid composite exhibited a considerably reduced attrition rate in comparison to the alloy. The inclusion of graphite and eggshell powder in the hybrid composite resulted in improved mechanical and tribological characteristics. These reinforcements offer a balanced improvement: graphite minimizes wear due to its lubricating effect, while eggshell strengthens the composite, improving both hardness and overall mechanical resilience. As the applied load and weight percentage increased, the composite demonstrated improved performance. The substantial reduction in wear rate attributed to the lubricating property of *Es* allowed the hybrid composite to operate effectively at higher velocities as well. This improvement implies that the hybrid composite can sustain prolonged service life in high-friction environments.

The CNC turning operations and AA6061-5%*Gr*-5%*Es* hybrid composite fabrication in accordance with Taguchi's L9 orthogonal array were successfully completed. By employing grey relational analysis, the optimal setting parameters were determined. The turning parameters that produced AA6061-5%*Gr*-5%*Es* hybrid composites at their optimal level were as follows: 1050 rpm cutting speed, 0.15 mm/rev feed, and 0.6mm depth of cut.

Based on the observations, it is possible to deduce that the hybrid composite that was created possesses enhanced mechanical and tribological characteristics, rendering it suitable for manufacturing in the aerospace and automotive sectors, including engine blocks, suspensions, pistons, and bearings.

7 REFERENCES

[1] Radha Krishnan, B., Theerkka Tharisanan, R., Arumuga Prabu, V., Immanuel, P., & Ramakrishnan, A. (2022). Experimental investigation of mechanical properties of Al7075-Al2O3-B4C composite via stir route. *Materials Today: Proceedings, 64*(5), 1721-1724. https://doi.org/10.1016/j.matpr.2022.05.498

[2] Pandiyarajan, R., Maran, P., Marimuthu, S., & Prabakaran, M. P. (2022). Investigation on mechanical properties of ZrO2, C and AA6061 metal matrix composites. *Advances in Materials and Processing Technologies, 8*(1), 178-186. https://doi.org/10.1080/2374068X.2020.1810946

[3] Ayalew Abebe, E., Devendra Kumar, S., Anil, K., & Anshul, Y. (2022). Fabrication and Characterization of Hybrid

Aluminium Al6061 Metal Matrix Composite Reinforced with SiC, B4C and MoS2 via Stir Casting. *International Journal of Metal casting.* https://doi.org/10.1007 /s40962-022-00800-1

[4] Kareem, A., Jaber Abu, Q., Asarudheen, A., Thanveer, A., & Aiman, Z. (2021). A Review on AA 6061 Metal Matrix Composites Produced by Stir Casting. *Materials (Basel), 14*(1), 175. https://doi.org/10.3390/ma14010175

[5] Mittal, P., Paswan, M. K., Sadasivuni, K. K., & Gupta, P. (2020). Structural, wear and thermal behaviour of Cu-Al2O3-graphite hybrid metal matrix composites. *Proceedings of the Institution of Mechanical Engineers, Part L: Journal of Materials: Design and Applications., 234*(8), 1154-1164. https://doi.org/10.1177/1464420720929377

[6] Hynes, N. R. J., Raja, S., Tharmaraj, R., Pruncu, C. I., & Dispinar, D. (2020). Mechanical and tribological characteristics of boron carbide reinforcement of AA6061 matrix composite. *Journal of the Brazilian Society of Mechanical Sciences and Engineering, 42*, 155. https://doi.org/10.1007/s40430-020-2237-2

[7] Karthikeyan, M., Devaraju, A., & Gopi, R. (2020). Investigations on mechanical properties of aluminium alloy Al6061 hybrid metal matrix composite. *Materials Today: Proceedings, 68*(5), 1504-1507. https://doi.org/10.1016/j.matpr.2022.07.130

[8] Venkatesan, S. P., Muthuswamy, G., Shyam Sundar, R., Ganesan, S., & Hemanandh, J. (2022). Investigation of mechanical properties of aluminum metal matrix composites with nanomaterial reinforcement. *Materials Today: Proceedings, 62*(2), 572-582. https://doi.org/10.1016/j.matpr.2022.03.594

[9] Dhanenthiran, M., Balamurugan, C., Senthil Kumar, N., Nagaprasad, N., Leta, T. J., Bayissa, B., Krishnaraj, R., Parthiban, K., Gunasekaran, M., & Nikolai, I. V. (2022). Experimental Investigation and Comparative Analysis of Aluminium Hybrid Metal Matrix Composites Reinforced with Silicon Nitride, Eggshell and Magnesium. *Materials, 15*(17). https://doi.org/10.3390/ma 15176098

[10] Satishkumar, P., Natarajan, N., Rajasekaran, S., Justin Maria Hillary, J., Biru B., Arnoldm C. A., Rey, Y. C., Vishnu, R., & Stephen, L. (2022). Investigation of Mechanical and Tribological Properties of AA6061/MWCNT/B4C Hybrid Metal Matrix Composite. *Advances in Materials Science and Engineering*, *2022*, 8. https://doi.org/10.1155/2022/ 1684169

[11] Tarun Kumar, K., Eshwar, D., Balakrishna, G., Sandeep Varma, K., Durga Prasad, B., & Sasivaradhan, S. (2022). Experimental Investigation on Metal Matrix Nanocomposite: Aluminium Alloy 6061 and 7075 with SiC and Fly Ash. *Journal of Nanomaterials, 2022*, 14. https://doi.org/10.1155 /2022/8368934

[12] Ibhadode, A. (2022). Engine Lightweighting: Use of Green Materials as Reinforcement in Aluminum Metal Matrix Composites. *Renewable Energy - Recent Advances, Intech Open*.

[13] Chandla, N. K., Kant, S., & Goud, M. M. (2021) Mechanical, tribological and microstructural characterization of stir cast Al-6061 metal/matrix composites a comprehensive review. *SādhanāIndian Academy of Sciences, 46*. https://doi.org/10.1007/s12046-021-01567-7

[14] Boppana, S. B., Dayanand, S., Murthy, B. V., Nagaral, M., Telagu, A., Kumar, V., & Auradi, V. (2021). Development and Mechanical Characterisation of Al6061-Al2O3-Graphene Hybrid Metal Matrix Composites. *Journal of Composites Science, 5*(6), 155. https://doi.org/10.3390/jcs5060155

[15] Olusesi, O. S. & Udoye, N. E. (2021) Development and characterization of AA6061 aluminium alloy /clay and rice husk ash composite. *Manufacturing Letters, 29*, 34-41. https://doi.org/10.1016/ jmfglet.2021.05.006

[16] Jayasathyakawin, S., Ravichandran, M., Ismail, S. O., & Srinivasan, D. (2023). Effects of hydroxyapatite addition on the microstructure and mechanical properties of sintered magnesium matrix composites. *Materials Today Communications, 35*, 1-19. https://doi.org/ 10.1016/j.mtcomm.2023.105582

[17] Singh, G. & Goyal, S. (2018). Dry sliding wear behaviour of AA6082-T6/SiC/B4C hybrid metal matrix composites using response surface methodology. *Proceedings of the Institution of Mechanical Engineers, Part L: Journal of Materials: Design and Applications, 232*(11), 952-964. https://doi.org/ 10.1177/1464420716657114

Contact Information:

M. DHANENTHIRAN, Mr., Assistant Professor,
(Corresponding author)
Department of Mechanical Engineering,
SRMTRP Engineering College (SRM Group),
Tiruchirappalli-621105
E-mail: dhanen.mohan@gmail.com

C. BALAMURUGAN, PhD, Professor
Department of Mechanical Engineering,
College of Engineering Guindy,
Anna University, Chennai - 600025
E-mail: balamurugan.c@annauniv.edu

A. BOVAS HERBERT BEJAXHIN, PhD, Associate Professor
Department of Mechanical Engineering Saveetha School of Engineering,
SIMATS, Chennai
E-mail: herbert.mech2007@gmail.com